Mechanical Systems and Signal Processing 226 (2025) 112294

Contents lists available at ScienceDirect

Mechanical Systems and Signal Processing

journal homepage: www.elsevier.com/locate/ymssp

Towards a single-loop Gaussian process regression based-active learning method for time-dependent reliability analysis

Chao Dang *, Marcos A. Valdebenito, Matthias G.R. Faes

Chair for Reliability Engineering, TU Dortmund University, Leonhard-Euler-Straße 5, 44227 Dortmund, Germany

ARTICLE INFO

Communicated by M. Beer

Keywords:
Time-dependent reliability analysis
Active learning
Gaussian process regression
Stopping criterion
Learning function

ABSTRACT

Time-dependent reliability analysis has received increasing attention for assessing the performance and safety of engineered components and systems subject to both random and time-varying dynamic factors. However, many existing methods may prove insufficient when applied to real-world problems, particularly in terms of applicability, efficiency and accuracy. This paper presents a novel time-dependent reliability analysis method called 'single-loop Gaussian process regression based-active learning' (SL-GPR-AL). In this method, a GPR model is trained as a global response surrogate model for the time-dependent performance function in an active learning fashion. A new stopping criterion is proposed to assess the convergence of the GPR model in estimating the time-dependent failure probability. Additionally, two new learning functions are introduced to identify the best next point for further refining the GPR model if the stopping criterion is not met. Finally, the well-trained GPR model in conjunction with Monte Carlo simulation provides the time-dependent failure probability over a specified time interval, along with the time-dependent failure probability function as a byproduct. Four numerical examples are analyzed to demonstrate the performance of the proposed method. The results indicate that our approach provides an alternative, efficient and accurate means for computationally expensive time-dependent reliability analysis.

1. Introduction

Reliability analysis aims to assess the likelihood that a component or system will perform its intended function without failure for a specified time period under given conditions, while taking into account various uncertainties. This makes it a critical aspect of modern engineering and applied sciences, particularly in assessing the performance and safety of components or systems. Depending on whether time-varying dynamic characteristics are considered, reliability analysis can be divided into time-independent (or time-invariant) reliability analysis and time-dependent (or time-variant) reliability analysis. In the former, the reliability of a component or system is assumed to be constant over time by ignoring time-dependent factors. In contrast, time-dependent reliability analysis accounts for the variation in reliability over time, considering factors such as corrosion, fatigue, deterioration, and environmental conditions that can affect the likelihood of failure as the component or system ages. In many real-world situations, the performance of a component or system changes over time, making time-dependent reliability analysis a more realistic approach. However, time-dependent reliability analysis is intuitively much more computationally involved than the time-independent one due to the additional consideration of the time scale. The existing methods for time-dependent reliability analysis can be broadly classified into three categories: (1) out-crossing rate methods, (2) composite limit state methods, and (3) extreme value methods. A brief overview of

* Corresponding author.
E-mail address: chao.dang@tu-dortmund.de (C. Dang).

https://doi.org/10.1016/j.ymssp.2024.112294
Received 19 September 2024; Received in revised form 2 December 2024; Accepted 29 December 2024
Available online 21 January 2025
0888-3270/© 2025 The Authors. Published by Elsevier Ltd. This is an open access article under the CC BY license (http://creativecommons.org/licenses/by/4.0/).

each is provided below, with more comprehensive discussions available in [1,2].

Out-crossing rate methods estimate the time-dependent failure probability by calculating the rate at which a component or system crosses a predefined failure threshold — transitioning from a safe state to a failure state — over a given time interval. Assuming all out-crossing events are statistically independent, Rice [3] first proposed what is now known as Rice formula, which expresses the time-dependent failure probability as an integral of the out-crossing rate over the time interval of interest. Since then, great efforts have been made to obtain the out-crossing rate, e.g., PHI2 [4], PHI2+ [5], moment-based PHI2 (MPHI2) [6], PHI2++ [7], analytical solutions [8,9], to name just a few. However, the independence assumption underlying these methods is often difficult to justify in practice, causing significant errors when the out-crossings are strongly dependent. To address this limitation, methods that account for statistical dependence between crossing events, such as joint out-crossing rates [10] and Markov process model [11], have been developed. Although considered the classical approach in time-dependent reliability analysis, out-crossing rate methods still face challenges in practical engineering applications.

Unlike out-crossing rate methods, composite limit state methods transform a time-dependent reliability problem into a conventional time-independent series-system reliability problem. Specifically, these methods discretize the original time-dependent performance function into a series of instantaneous performance functions evaluated at discrete time nodes. By doing so, the time-dependent failure probability can be obtained by analyzing the failure probability of the series system. Examples of composite limit state methods include the first-order reliability method (FORM) [12–15], importance sampling [16,17], subset simulation [18–20], and line sampling [21,22]. These FORM-based methods can become computationally demanding when the number of time nodes is large and naturally inherit limitations of FORM. On the other hand, most stochastic simulation-based methods can offer better accuracy and broader applicability compared to FORM, but at the cost of a large number of performance function evaluations.

As an alternative approach to time-dependent reliability analysis, extreme value methods transform the time-dependent problem into a time-independent one. More precisely, the time-dependent failure probability is equivalent to the probability that the extreme value distribution of the performance function's response is below (or above) the failure threshold over the time interval of interest. This transformation allows time-dependent reliability analysis to be effectively addressed using well-established time-invariant reliability analysis methods, as demonstrated in studies such as [23–25]. In addition, active learning Kriging methods have gained increasing attention for time-dependent reliability analysis. These methods can be categorized into double-loop and single-loop schemes. In the double-loop scheme, a Kriging model is constructed for the extreme value response of the performance function in the outer loop, while the inner loop identifies the extreme value for each time trajectory using another Kriging model, both potentially implemented in an active learning manner. Typical examples include the nested extreme response surface approach [26,27], mixed efficient global optimization (EGO) method [28], active learning Kriging (AK) coupled with importance sampling (AK-co-IS) and AK coupled with subset simulation (AK-co-SS) [29], parallel EGO method [30], double-loop Kriging combined with importance sampling (DLK-IS) method [31], etc. As a more straightforward alternative, the single-loop scheme directly builds a global Kriging model for the performance function using active learning. Notable examples include the single-loop Kriging (SILK) method [32], equivalent stochastic process transformation (eSPT) method [33], active failure-pursuing Kriging (AFPK) method [34], real-time estimation error-guided active learning Kriging (REAL) method [35], and several others [36–42]. Compared to the double-loop scheme, the single-loop approach typically requires fewer evaluations of the actual performance function. However, it still has certain limitations, particularly in key components of active learning methods, such as the surrogate model, the reliability analysis algorithm, the stopping criterion, and the learning function. Each of these aspects presents opportunities for further improvement.

To partially address the research gap identified above, this work introduces a new single-loop Gaussian process regression-based active learning (SL-GPR-AL) method for computationally expensive time-dependent reliability analysis. This method is versatile, as: (1) it can be applied to performance functions, regardless of whether they are subject to stochastic processes, and (2) it provides both the time-dependent failure probability over a given time interval and insights into the evolution of the failure probability as a byproduct. The main contributions of this work can be summarized as follows. First, a new stopping criterion is introduced as a key element of active learning, providing a measure of convergence for the GPR model. Second, two new learning functions are developed—another critical component of active learning—that guide the selection of the most informative points for further refining the GPR model when the stopping criterion is not met.

The rest of this paper is structured as follows. Section 2 provides some background information on this study. The proposed SL-GPR-AL method is introduced in Section 3. Four numerical examples are investigated in Section 4 to demonstrate the proposed method. Some concluding remarks are given in Section 5.

2. Preliminaries

This section presents the basic concepts and notations that are essential for understanding and developing the main results of this paper. First, we define the time-dependent failure probabilities that are of interest in time-dependent reliability analysis in Section 2.1. Then, we introduce the discretization of stochastic processes in Section 2.2. Finally, we describe the SL-GPR for time-dependent failure probability analysis in Section 2.3 that underpins our main development.

2.1. Definition of time-dependent failure probabilities

In general, time-dependent reliability analysis problems can be abstracted in several different forms. In the following, we will consider a relatively general case. Let $\boldsymbol{X} = [X_1, X_2, \dots, X_{d_1}] \in \mathcal{X} \subseteq \mathbb{R}^{d_1}$ denote a vector of d_1 random variables with support $\mathcal{X}$ and $\boldsymbol{Y}(\tau) = [Y_1(\tau), Y_2(\tau), \dots, Y_{d_2}(\tau)] \in \mathcal{Y} \subseteq \mathbb{R}^{d_2}$ denote a vector of d_2 stochastic processes with support $\mathcal{Y}$. The so-called

performance function (also known as the limit state function) can be written as $g(\boldsymbol{X}, \boldsymbol{Y}(\tau), \tau)$, where $\tau \in [t_0, t_f]$ represents the temporal parameter (t_0 and t_f denote the initial and final times, respectively). It is assumed that the performance function g can be evaluated instantaneously for any given $(\boldsymbol{x}, \boldsymbol{y}(\tau), \tau)$. The underlying component or system is considered to have failed if the performance function takes a negative value at any time within the considered time interval (i.e., the first-passage failure). Therefore, the time-dependent failure probability of interest is mathematically defined as:

$$P_f(t_0, t_f) = \mathbb{P}\left\{g(\boldsymbol{X}, \boldsymbol{Y}(\tau), \tau) < 0, \exists \tau \in [t_0, t_f]\right\}, \tag{1}$$

where $\mathbb{P}$ is the probability operator; $\exists$ means 'there exists'. In addition to $P_f(t_0, t_f)$, one may also be interested in the failure probability function indexed by $t \in [t_0, t_f]$:

$$P_f(t_0, t) = \mathbb{P}\left\{g(\boldsymbol{X}, \boldsymbol{Y}(\tau), \tau) < 0, \exists \tau \in [t_0, t]\right\}, \tag{2}$$

which reflects how the failure probability varies with time over the reference period $[t_0, t_f]$. It is noted that $P_f(t_0, t_f)$ is the final value of $P_f(t_0, t)$, i.e., $P_f(t_0, t_f) = P_f(t_0, t = t_f)$. This implies that $P_f(t_0, t_f)$ can be obtained straightforwardly once $P_f(t_0, t)$ is available. In practice, however, deriving an analytical solution of $P_f(t_0, t)$ is usually intractable, even for $P_f(t_0, t_f)$. Therefore, efficient and accurate approximation or numerical methods are relevant for solving $P_f(t_0, t_f)$ and $P_f(t_0, t)$. Intuitively, the latter would require more computational effort. For numerical purposes, the time interval $[t_0, t_f]$ needs to be discretized. In this study, we discretize $[t_0, t_f]$ into equally spaced n_t time points, i.e., $t_0, t_1, t_2, \ldots, t_{n_t-2}, t_f$, where $t_k = t_0 + \kappa \Delta t$ and $\Delta t = \frac{t_f - t_0}{n_t - 1}$ for $\kappa = 0, 1, \ldots, n_t - 1$.

2.2. Discretization of stochastic processes

In addition to time discretization, it is often also necessary to discretize the stochastic processes $\boldsymbol{Y}(\tau)$. This involves approximating a stochastic process with a finite set of random variables. For this purpose, many techniques are available in the literature, such as Karhunen–Loève (K–L) expansion [43], expansion optimal linear estimation [44], spectral representation method [45] and stochastic harmonic function representation [46], etc. In this study, the K–L expansion is used as an illustrative example. Consider a second-order stochastic process $Y(\tau)$, where the subscript is omitted. It can be approximated using the K–L expansion:

$$\hat{Y}(\tau) = \mu_Y(\tau) + \sum_{r=1}^{n_{\mathrm{KL}}} \sqrt{\lambda_r} \xi_r \varphi_r(\tau), \tag{3}$$

where $\mu_Y(\tau)$ is the mean function of $Y(\tau)$; n_{KL} is the number of truncation terms; λ_r and $\varphi_r(\tau)$ are the rth dominated eigenvalue and the corresponding eigenvector of the covariance matrix $\boldsymbol{C}$ with its (i, j)-th entry being $[\boldsymbol{C}]_{i+1,j+1} = \sigma_Y(t_i)\sigma_Y(t_j)\rho_Y(t_i, t_j)$, $i = 0, 1, \ldots, n_t - 1$, $j = 0, 1, \ldots, n_t - 1$; $\sigma_Y(\tau)$ is the standard deviation function of $Y(\tau)$; $\rho_Y(t_1, t_2)$ is the auto-correlation coefficient function of $Y(\tau)$; $\left\{\xi_j\right\}_{j=1}^{n_{\mathrm{KL}}}$ is a set of n_{KL} uncorrelated standardized random variables. If $Y(\tau)$ is Gaussian, then $\left\{\xi_j\right\}_{j=1}^{n_{\mathrm{KL}}}$ are independent standard Gaussian random variables. The number of truncation terms n_{KL} can be determined by the explained variance ratio:

$$\frac{\sum_{r=1}^{n_{\mathrm{KL}}} \lambda_j}{\sum_{r=1}^{n_t} \lambda_j} \geq \delta_{\mathrm{KL}}, \tag{4}$$

where δ_{KL} is a user-specified threshold. Note that other suitable stochastic process discretization techniques can also be applied to the proposed method presented in Section 3.

2.3. SL-GPR for time-dependent failure probability analysis

GPR [47] is a powerful non-parametric Bayesian approach to regression. It has been widely used in machine learning and many other fields because of its flexibility and inherent ability to quantify uncertainty over predictions. For these reasons, we use the GPR technique as a probabilistic global surrogate model for time-dependent reliability analysis in this study, as briefly described below. More details about the GPR can be found in the cited reference.

Before observing any data, it is assumed that our prior beliefs about the performance function g can be expressed by a Gaussian process (GP) prior:

$$\hat{g}_0(\boldsymbol{x}, \hat{\boldsymbol{y}}(\tau), \tau) \sim \mathcal{GP}(m_0(\boldsymbol{x}, \hat{\boldsymbol{y}}(\tau), \tau), k_0(\boldsymbol{x}, \hat{\boldsymbol{y}}(\tau), \tau, \boldsymbol{x}', \hat{\boldsymbol{y}}'(\tau'), \tau')), \tag{5}$$

where $\hat{g}_0(\boldsymbol{x}, \hat{\boldsymbol{y}}(\tau), \tau)$ denotes the prior distribution of $g(\boldsymbol{x}, \hat{\boldsymbol{y}}(\tau), \tau)$; $m_0(\boldsymbol{x}, \hat{\boldsymbol{y}}(\tau), \tau)$ and $k_0(\boldsymbol{x}, \hat{\boldsymbol{y}}(\tau), \tau, \boldsymbol{x}', \hat{\boldsymbol{y}}'(\tau'), \tau')$ are the prior mean and covariance functions, respectively. The prior mean function specifies the expected value of g, while the prior covariance function determines the smoothness and other properties of g before any data are observed.

After observing data $\boldsymbol{\mathcal{D}} = \{\boldsymbol{\mathcal{U}}, \boldsymbol{\mathcal{Z}}\}$ (where $\boldsymbol{\mathcal{U}} = \left\{\boldsymbol{\mathcal{X}}, \hat{\boldsymbol{\mathcal{Y}}}(\boldsymbol{\tau}), \boldsymbol{\tau}\right\} = \left\{\boldsymbol{x}^{(i)}, \hat{\boldsymbol{y}}^{(i)}(\tau^{(i)}), \tau^{(i)}\right\}_{i=1}^{n}$ and $\boldsymbol{\mathcal{Z}} = \left\{g(\boldsymbol{x}^{(i)}, \hat{\boldsymbol{y}}^{(i)}(\tau^{(i)}), \tau^{(i)}\right\}_{i=1}^{n}$), conditioning the GP prior on $\boldsymbol{\mathcal{D}}$ gives a GP posterior for g:

$$\hat{g}_n(\boldsymbol{x}, \hat{\boldsymbol{y}}(\tau), \tau) \sim \mathcal{GP}(m_n(\boldsymbol{x}, \hat{\boldsymbol{y}}(\tau), \tau), k_n(\boldsymbol{x}, \hat{\boldsymbol{y}}(\tau), \tau, \boldsymbol{x}', \hat{\boldsymbol{y}}'(\tau'), \tau')), \tag{6}$$

where $\hat{g}_n(\boldsymbol{x}, \hat{\boldsymbol{y}}(\tau), \tau)$ denotes the posterior distribution of g; $m_n(\boldsymbol{x}, \hat{\boldsymbol{y}}(\tau), \tau)$ and $k_n(\boldsymbol{x}, \hat{\boldsymbol{y}}(\tau), \tau, \boldsymbol{x}', \hat{\boldsymbol{y}}'(\tau'), \tau')$ are the posterior mean and covariance functions respectively, which are readily available in analytic form:

$$m_n(\boldsymbol{x}, \hat{\boldsymbol{y}}(\tau), \tau) = m_0(\boldsymbol{x}, \hat{\boldsymbol{y}}(\tau), \tau) + \boldsymbol{k}_0(\boldsymbol{x}, \hat{\boldsymbol{y}}(\tau), \tau, \boldsymbol{\mathcal{U}})^{\top} \boldsymbol{K}_0^{-1}(\boldsymbol{\mathcal{Z}} - \boldsymbol{m}_0(\boldsymbol{\mathcal{U}})), \tag{7}$$

$$k_n(\boldsymbol{x}, \hat{\boldsymbol{y}}(\tau), \tau, \boldsymbol{x}', \hat{\boldsymbol{y}}'(\tau'), \tau') = k_0(\boldsymbol{x}, \hat{\boldsymbol{y}}(\tau), \tau, \boldsymbol{x}', \hat{\boldsymbol{y}}'(\tau'), \tau') - \boldsymbol{k}_0(\boldsymbol{x}, \hat{\boldsymbol{y}}(\tau), \tau, \boldsymbol{\mathcal{U}})^{\top} \boldsymbol{K}_0^{-1} \boldsymbol{k}_0(\boldsymbol{\mathcal{U}}, \boldsymbol{x}', \hat{\boldsymbol{y}}'(\tau'), \tau'), \tag{8}$$

where $\boldsymbol{m}_0(\boldsymbol{\mathcal{U}})$ is an n-by-1 mean vector with its ith element being $m_0(\boldsymbol{\mathcal{U}}^{(i)})$; $\boldsymbol{k}_0(\boldsymbol{x}, \hat{\boldsymbol{y}}(\tau), \tau, \boldsymbol{\mathcal{U}})$ is an n-by-1 covariance vector with its ith element being $k_0(\boldsymbol{x}, \hat{\boldsymbol{y}}(\tau), \tau, \boldsymbol{\mathcal{U}}^{(i)})$; $\boldsymbol{k}_0(\boldsymbol{\mathcal{U}}, \boldsymbol{x}', \hat{\boldsymbol{y}}'(\tau'), \tau')$ is also an n-by-1 covariance vector with its ith element being $k_0(\boldsymbol{\mathcal{U}}^{(i)}, \boldsymbol{x}', \hat{\boldsymbol{y}}'(\tau'), \tau')$; $\boldsymbol{K}_0$ is an n-by-n covariance matrix with its (i, j)-th entry being $\left[\boldsymbol{K}_0\right]_{i,j} = k_0(\boldsymbol{\mathcal{U}}^{(i)}, \boldsymbol{\mathcal{U}}^{(j)})$. The GP posterior provides not only a mean prediction $m_n(\boldsymbol{x}, \hat{\boldsymbol{y}}(\tau), \tau)$, but also a measure of uncertainty in the prediction for the g-function value at an unseen point $(\boldsymbol{x}, \hat{\boldsymbol{y}}(\tau), \tau)$, given by the posterior variance $\sigma_n^2(\boldsymbol{x}, \hat{\boldsymbol{y}}(\tau), \tau) = k_n(\boldsymbol{x}, \hat{\boldsymbol{y}}(\tau), \tau, \boldsymbol{x}, \hat{\boldsymbol{y}}(\tau), \tau)$.

The time-dependent failure probability $P_f(t_0, t_f)$ can be estimated from the posterior mean prediction via Monte Carlo simulation (MCS):

$$\hat{P}_{f,n}(t_0, t_f) = \frac{1}{N} \sum_{j=1}^{N} I(\min_{k=0}^{n_t-1} m_n(\boldsymbol{x}^{(j)}, \hat{\boldsymbol{y}}^{(j)}(t_k), t_k) < 0), \tag{9}$$

where N is the number of samples; $\left\{\boldsymbol{x}^{(j)}\right\}_{j=1}^{N}$ is a set of N random samples of $\boldsymbol{X}$; $\left\{\hat{\boldsymbol{y}}^{(j)}(t_k)\right\}_{j=1}^{N}$ is a set of N random samples of $\hat{Y}(t_k)$, which can be generated using the K–L expansion; $I(\cdot)$ is the indicator function: it returns one if its argument is true, zero otherwise. The associated coefficient of variation (CoV) is given by:

$$\widehat{CoV}_{\hat{P}_{f,n}(t_0,t_f)} = \sqrt{\frac{1 - \hat{P}_{f,n}(t_0, t_f)}{(N-1)\hat{P}_{f,n}(t_0, t_f)}}. \tag{10}$$

Similarly, the time-dependent failure probability function $P_f(t_0, t)$ can also be evaluated in a pointwise manner:

$$\hat{P}_{f,n}(t_0, t_\kappa) = \frac{1}{N} \sum_{j=1}^{N} I(\min_{q=0}^{\kappa} m_n(\boldsymbol{x}^{(j)}, \hat{\boldsymbol{y}}^{(j)}(t_q), t_q) < 0), \kappa = 0, 1, \ldots, n_t - 1. \tag{11}$$

The corresponding CoVs can be expressed as:

$$\widehat{CoV}_{\hat{P}_{f,n}(t_0,t_\kappa)} = \sqrt{\frac{1 - \hat{P}_{f,n}(t_0, t_\kappa)}{(N-1)\hat{P}_{f,n}(t_0, t_\kappa)}}, \kappa = 0, 1, \ldots, n_t - 1. \tag{12}$$

Note that the above SL-GPR model can predict the time-dependent failure probability $\hat{P}_{f,n}(t_0, t_f)$ as well as $\hat{P}_{f,n}(t_0, t_\kappa)$ using MCS, given the data $\boldsymbol{\mathcal{D}}$. Consequently, the number of data points and the locations of $\boldsymbol{\mathcal{U}}$ can significantly affect the performance (e.g., accuracy and efficiency) of the SL-GPR method. This concern motivates the development reported in the following section.

3. Proposed SL-GPR-AL method

In this section, we present the proposed SL-GPR-AL method for time-dependent reliability analysis. In Section 3.1, an overview of the proposed method is given. This is followed by the stopping criterion and learning functions in Sections 3.2 and 3.3, respectively. The procedure for implementing the proposed method is summarized in Section 3.4.

3.1. Overview of the proposed method

As the name suggests, the key idea behind the proposed SL-GPR-AL method is to integrate AL with SL-GPR (as explained in Section 2.3) for time-dependent reliability analysis. It starts with a small initial set of training data consisting $n = n_0$ input–output pairs of the g-function, i.e., $\boldsymbol{\mathcal{D}} = \{\boldsymbol{\mathcal{U}}, \boldsymbol{\mathcal{Z}}\}$, which is used to build a GPR model $\hat{g}_n(\boldsymbol{x}, \hat{\boldsymbol{y}}(\tau), \tau)$. Time-dependent failure probabilities $\hat{P}_{f,n}(t_0, t_\kappa)$ are then calculated using this model. The method checks whether a stopping criterion is met, such as achieving a desired accuracy. If not, the method identifies the best next point $\boldsymbol{u}^{(n+1)}$ for improving the prediction of the GPR via a learning function, evaluates the corresponding g-function output $z^{(n+1)}$, updates the training data via $\boldsymbol{\mathcal{D}} = \boldsymbol{\mathcal{D}} \cup \left\{\boldsymbol{u}^{(n+1)}, z^{(n+1)}\right\}$. The iterative process repeats until the stopping criterion is satisfied. The general workflow of the proposed method is shown in Fig. 1. Note that in this study our main focus is on the time-dependent failure probability $\hat{P}_{f,n}(t_0, t_f)$ rather than the failure probability function $\hat{P}_{f,n}(t_0, t_k)$, but the latter can be obtained as a byproduct.

3.2. Stopping criterion and its numerical treatment

A key ingredient in the proposed SL-GPR-AL method is the stopping criterion, which determines the condition under which the iterative process should be terminated. In general, a stopping criterion can be designed based on several considerations, such as convergence, iteration limits, error tolerance, resource constraints, and a combination thereof. In this study, we are mainly concerned with developing a convergence-based stopping criterion.

Recall that the predictive model given by the SL-GPR model conditional on data $\boldsymbol{\mathcal{D}}$ is a GP, i.e., $\hat{g}_n(\boldsymbol{x}, \hat{\boldsymbol{y}}(\tau), \tau)$. The posterior mean function $m_n(\boldsymbol{x}, \hat{\boldsymbol{y}}(\tau), \tau)$ is used as a surrogate for the true g-function to predict the time-dependent failure probability:

$$P_{f,n}(t_0, t_f) = \mathbb{P}\left\{m_n(\boldsymbol{X}, \hat{\boldsymbol{Y}}(\tau), \tau) < 0, \exists \tau \in [t_0, t_f]\right\} = \mathbb{P}\left\{\min_{\tau \in [t_0, t_f]} m_n(\boldsymbol{X}, \hat{\boldsymbol{Y}}(\tau), \tau) < 0\right\}. \tag{13}$$

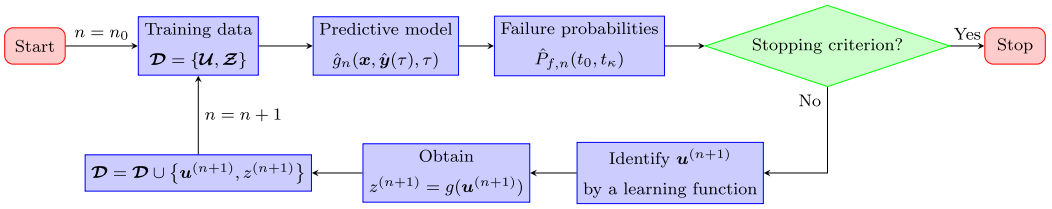


Fig. 1. General workflow of the proposed SL-GPR-AL method.

By appealing to the credible bounds $\left[m_n(\boldsymbol{x}, \hat{\boldsymbol{y}}(\tau), \tau) - b\sigma_n(\boldsymbol{x}, \hat{\boldsymbol{y}}(\tau), \tau), m_n(\boldsymbol{x}, \hat{\boldsymbol{y}}(\tau), \tau) + b\sigma_n(\boldsymbol{x}, \hat{\boldsymbol{y}}(\tau), \tau)\right]$ of $\hat{g}_n$ (where $b > 0$ is the credibility coefficient), the following two quantities can be defined:

$$\begin{aligned} P^+_{f,n}(t_0, t_f) =& \mathbb{P}\left\{m_n(\boldsymbol{X}, \hat{\boldsymbol{Y}}(\tau), \tau) - b\sigma_n(\boldsymbol{X}, \hat{\boldsymbol{Y}}(\tau), \tau) < 0, \exists \tau \in [t_0, t_f]\right\} \\ =& \mathbb{P}\left\{\min_{\tau \in [t_0, t_f]} m_n(\boldsymbol{X}, \hat{\boldsymbol{Y}}(\tau), \tau) - b\sigma_n(\boldsymbol{X}, \hat{\boldsymbol{Y}}(\tau), \tau) < 0\right\}, \end{aligned} \tag{14}$$

$$\begin{aligned} P^-_{f,n}(t_0, t_f) =& \mathbb{P}\left\{m_n(\boldsymbol{X}, \hat{\boldsymbol{Y}}(\tau), \tau) + b\sigma_n(\boldsymbol{X}, \hat{\boldsymbol{Y}}(\tau), \tau) < 0, \exists \tau \in [t_0, t_f]\right\} \\ =& \mathbb{P}\left\{\min_{\tau \in [t_0, t_f]} m_n(\boldsymbol{X}, \hat{\boldsymbol{Y}}(\tau), \tau) + b\sigma_n(\boldsymbol{X}, \hat{\boldsymbol{Y}}(\tau), \tau) < 0\right\}, \end{aligned} \tag{15}$$

where $P^+_{f,n}(t_0, t_f)$ and $P^-_{f,n}(t_0, t_f)$ can be interpreted as the time-dependent failure probabilities by replacing the true g-function with the lower and upper credible bounds of $\hat{g}_n$, respectively. The difference between $P^-_{f,n}(t_0, t_f)$ and $P^+_{f,n}(t_0, t_f)$ measures our epistemic uncertainty about $P_{f,n}(t_0, t_f)$, as the time-dependent failure probability estimate. Theoretically speaking, $P_{f,n}(t_0, t_f)$ converges towards the true time-dependent failure probability $P_f(t_0, t_f)$ when $P^-_{f,n}(t_0, t_f) \to P^+_{f,n}(t_0, t_f)$ (or $P^+_{f,n}(t_0, t_f) \to P^-_{f,n}(t_0, t_f)$).

The stopping criterion proposed in this study takes the form:

$$\frac{|P^+_{f,n}(t_0, t_f) - P^-_{f,n}(t_0, t_f)|}{P_{f,n}(t_0, t_f)} < \epsilon, \tag{16}$$

where ϵ is a user-prescribed threshold. This criterion indicates that the iteration will stop when the absolute difference between $P^+_{f,n}(t_0, t_f)$ and $P^-_{f,n}(t_0, t_f)$ relative to $P_{f,n}(t_0, t_f)$ falls below the threshold ϵ. A smaller ϵ may lead to a more accuracy estimate of the time-dependent failure probability, albeit at the cost of an increased number of g-function evaluations, and vice versa. The proposed stopping criterion can be seen as an extension of the stopping criterion [48] from time-independent reliability analysis to time-dependent reliability analysis. In the latter context, a similar but slightly different stopping criterion can be found in [49].

In the practical implementation of the proposed stopping criterion, the three terms $P_{f,n}(t_0, t_f)$, $P^+_{f,n}(t_0, t_f)$ and $P^-_{f,n}(t_0, t_f)$ have to be calculated numerically. Similar to the first term (as outlined in Section 2.3), the last two terms are also calculated using MCS. The estimators of $P^+_{f,n}(t_0, t_f)$ and $P^-_{f,n}(t_0, t_f)$ are given by:

$$\hat{P}^+_{f,n}(t_0, t_f) = \frac{1}{N}\sum_{j=1}^{N} I(\min_{\kappa=0}^{n_t-1} m_n(\boldsymbol{x}^{(j)}, \hat{\boldsymbol{y}}^{(j)}(t_\kappa), t_\kappa) - b\sigma_n(\boldsymbol{x}^{(j)}, \hat{\boldsymbol{y}}^{(j)}(t_k), t_\kappa) < 0), \tag{17}$$

$$\hat{P}^-_{f,n}(t_0, t_f) = \frac{1}{N}\sum_{j=1}^{N} I(\min_{\kappa=0}^{n_t-1} m_n(\boldsymbol{x}^{(j)}, \hat{\boldsymbol{y}}^{(j)}(t_\kappa), t_\kappa) + b\sigma_n(\boldsymbol{x}^{(j)}, \hat{\boldsymbol{y}}^{(j)}(t_\kappa), t_\kappa) < 0). \tag{18}$$

The associated CoVs of $\hat{P}^+_{f,n}(t_0, t_f)$ and $\hat{P}^-_{f,n}(t_0, t_f)$ are expressed as:

$$\widehat{CoV}_{\hat{P}^+_{f,n}(t_0,t_f)} = \sqrt{\frac{1 - \hat{P}^+_{f,n}(t_0, t_f)}{(N-1)\hat{P}^+_{f,n}(t_0, t_f)}}, \tag{19}$$

$$\widehat{CoV}_{\hat{P}^-_{f,n}(t_0,t_f)} = \sqrt{\frac{1 - \hat{P}^-_{f,n}(t_0, t_f)}{(N-1)\hat{P}^-_{f,n}(t_0, t_f)}}. \tag{20}$$

Remark 1. An alternative stopping criterion can be defined as $\frac{|P^+_{f,n}(t_0,t_f) - P_{f,n}(t_0,t_f)|}{P_{f,n}(t_0,t_f)} < \epsilon$ or $\frac{|P_{f,n}(t_0,t_f) - P^-_{f,n}(t_0,t_f)|}{P_{f,n}(t_0,t_f)} < \epsilon$. However, these alternatives are not further explored in this study.

3.3. Learning functions and the best next point selection

Another critical component of the proposed SL-GPR-AL method is the learning function (often referred to as the acquisition function or query strategy), which guides the selection of the most informative point at which to evaluate the true g function when the stopping criterion is not met. It therefore directly affects the performance of the resulting method. In this study, a new query strategy is developed.

Remember that the SL-GPR model, conditional on the data $\mathcal{D}$, yields a GP posterior $\hat{g}_n(\boldsymbol{x}, \hat{\boldsymbol{y}}(\tau), \tau)$, which is used to estimate the time-dependent failure probability $P_f(t_0, t_f)$. At each point $(\boldsymbol{x}, \hat{\boldsymbol{y}}(\tau), \tau)$, the predictive distribution of g follows a Gaussian distribution $\mathcal{N}(m_n(\boldsymbol{x}, \hat{\boldsymbol{y}}(\tau), \tau), \sigma_n^2(\boldsymbol{x}, \hat{\boldsymbol{y}}(\tau), \tau))$. For predicting the time-dependent failure probability, it might be more important to accurately predict the sign of the performance function than its exact values. If we use the posterior mean function to predict the sign of g, there is a chance that the sign is predicted incorrectly. The associated probability of misjudgment (PoM) is given by [50]:

$$PoM(\boldsymbol{x}, \hat{\boldsymbol{y}}(\tau), \tau) = \boldsymbol{\Phi}\left(-\frac{|m_n(\boldsymbol{x}, \hat{\boldsymbol{y}}(\tau), \tau)|}{\sigma_n(\boldsymbol{x}, \hat{\boldsymbol{y}}(\tau), \tau)}\right). \tag{21}$$

The PoM function quantifies the likelihood that the predicted sign of the true performance function g is wrong, considering the current uncertainty in the model's prediction. Furthermore, we can also define a weighted PoM (WPoM) function such that:

$$WPoM(\boldsymbol{x}, \hat{\boldsymbol{y}}(\tau), \tau) = \boldsymbol{\Phi}\left(-\frac{|m_n(\boldsymbol{x}, \hat{\boldsymbol{y}}(\tau), \tau)|}{\sigma_n(\boldsymbol{x}, \hat{\boldsymbol{y}}(\tau), \tau)}\right) f_{\boldsymbol{X}}(\boldsymbol{x}) f_{\hat{\boldsymbol{Y}}(\tau)}(\hat{\boldsymbol{y}}(\tau)), \tag{22}$$

where $f_{\boldsymbol{X}}(\boldsymbol{x})$ is the joint probability density function (PDF) of $\boldsymbol{X}$; $f_{\hat{\boldsymbol{Y}}(\tau)}(\hat{\boldsymbol{y}}(\tau))$ is the joint PDF of $\hat{\boldsymbol{Y}}(\tau)$ at the time instant τ. The WPoM function takes into account both the uncertainty in the model's predictions and the likelihood of specific input scenarios. It can be seen as a direct extension of the learning function (see, e.g., [51,52]) developed in the context of time-independent reliability analysis. Additionally, we can define an integrated PoM (IPoM) function:

$$IPoM(\tau) = \int_{\mathcal{Y}(\tau)} \int_{\mathcal{X}} \boldsymbol{\Phi}\left(-\frac{|m_n(\boldsymbol{x}, \hat{\boldsymbol{y}}(\tau), \tau)|}{\sigma_n(\boldsymbol{x}, \hat{\boldsymbol{y}}(\tau), \tau)}\right) f_{\boldsymbol{X}}(\boldsymbol{x}) f_{\hat{\boldsymbol{Y}}(\tau)}(\hat{\boldsymbol{y}}(\tau)) \mathrm{d}\boldsymbol{x} \mathrm{d}\hat{\boldsymbol{y}}(\tau), \tag{23}$$

where $\mathcal{Y}(\tau)$ denotes the support of $\hat{\boldsymbol{Y}}(\tau)$ at the time instant τ. The IPoM function quantifies the overall risk of making incorrect sign predictions across all possible input scenarios at a specific time instant.

After defining these learning functions, the next best point $\left(\boldsymbol{x}^{(n+1)}, \hat{\boldsymbol{y}}^{(n+1)}(\tau^{(n+1)}), \tau^{(n+1)}\right)$ at which to evaluate the g function can be identified following a two-step procedure. In the first step, the best next time $\tau^{(n+1)}$ is selected by maximizing the estimated IPoM function:

$$\tau^{(n+1)} = \underset{\tau \in [t_0, t_f]}{\operatorname{argmax}} \widehat{IPoM}(\tau), \tag{24}$$

where $\widehat{IPoM}(\tau)$ is obtained by applying MCS:

$$\widehat{IPoM}(\tau) = \frac{1}{N} \sum_{j=1}^{N} \boldsymbol{\Phi}\left(-\frac{|m_n(\boldsymbol{x}^{(j)}, \hat{\boldsymbol{y}}^{(j)}(\tau), \tau)|}{\sigma_n(\boldsymbol{x}^{(j)}, \hat{\boldsymbol{y}}^{(j)}(\tau), \tau)}\right). \tag{25}$$

In the second step, we identify the best next point $\left(\boldsymbol{x}^{(n+1)}, \hat{\boldsymbol{y}}^{(n+1)}(\tau^{(n+1)})\right)$ by maximizing the WPoM function conditional on $\tau = \tau^{(n+1)}$:

$$\left(\boldsymbol{x}^{(n+1)}, \hat{\boldsymbol{y}}^{(n+1)}(\tau^{(n+1)})\right) = \underset{\boldsymbol{x} \in \left\{\boldsymbol{x}^{(j)}\right\}_{j=1}^{N}, \hat{\boldsymbol{y}}^{(n+1)}(\tau^{(n+1)}) \in \left\{\hat{\boldsymbol{y}}^{(j)}(\tau^{(n+1)})\right\}_{j=1}^{N}}{\operatorname{argmax}} WPoM(\boldsymbol{x}, \hat{\boldsymbol{y}}(\tau^{(n+1)}), \tau^{(n+1)}). \tag{26}$$

3.4. Implementation procedure of the proposed method

The procedure for implementing the proposed SL-GPR-AL method for time-dependent reliability analysis is summarized below, along with a flowchart shown in Fig. 2.

Step 1: Discretize the time period of interest

Discretize the time period of interest $[t_0, t_f]$ into equally spaced n_t time points, i.e., $t_0, t_1, t_2, \ldots, t_{n_t-2}, t_f$, where $t_\kappa = t_0 + \kappa \Delta t$ and $\Delta t = \frac{t_f - t_0}{n_t - 1}$ for $\kappa = 0, 1, \ldots, n_t - 1$.

Step 2: Generate an initial sample pool

Generate an initial sample pool $\mathcal{S} = \left\{\boldsymbol{x}^{(j)}, \hat{\boldsymbol{y}}^{(j)}(t_\kappa), t_\kappa\right\}_{j=1,\kappa=0}^{N, n_t-1}$, where $\left\{\boldsymbol{x}^{(j)}\right\}_{j=1}^{N}$ is an N-by-d_1 matrix consisting of a random sample of $\boldsymbol{X}$ generated according to $f_{\boldsymbol{X}}(\boldsymbol{x})$ and $\left\{\hat{\boldsymbol{y}}^{(j)}(t_\kappa)\right\}_{j=1}^{N}$ is an N-by-d_2 matrix consisting of a random sample of $\boldsymbol{Y}(\tau)$ at $\tau = t_\kappa$ generated using K–L expansion.

Step 3: Generate an initial training dataset

Generate an initial training dataset $\mathcal{D} = \{\mathcal{U}, \mathcal{Z}\}$, where $\mathcal{U} = \left\{\mathcal{X}, \hat{\mathcal{Y}}(\boldsymbol{\tau}), \boldsymbol{\tau}\right\} = \left\{\boldsymbol{x}^{(i)}, \hat{\boldsymbol{y}}^{(i)}(\tau^{(i)}), \tau^{(i)}\right\}_{i=1}^{n_0}$ and $\mathcal{Z} = \left\{g(\boldsymbol{x}^{(i)}, \hat{\boldsymbol{y}}^{(i)}(\tau^{(i)}), \tau^{(i)})\right\}_{i=1}^{n_0}$. In this study, $\boldsymbol{\tau} = \left\{\tau^{(i)}\right\}_{i=1}^{n_0}$ are n_0 evenly distributed time nodes over $[t_0, t_f]$. Furthermore, $\mathcal{X} = \left\{\boldsymbol{x}^{(i)}\right\}_{i=1}^{n_0}$ are drawn from $f_{\boldsymbol{X}}(\boldsymbol{x})$ using Hammersley sequence, and $\hat{\mathcal{Y}}(\boldsymbol{\tau}) = \left\{\hat{\boldsymbol{y}}^{(i)}(\tau^{(i)})\right\}_{i=1}^{n_0}$ are drawn from $f_{\hat{\boldsymbol{Y}}(\tau)}(\hat{\boldsymbol{y}}(\tau))$ using K–L expansion in conjunction with Hammersley sequence. Let $n = n_0$.

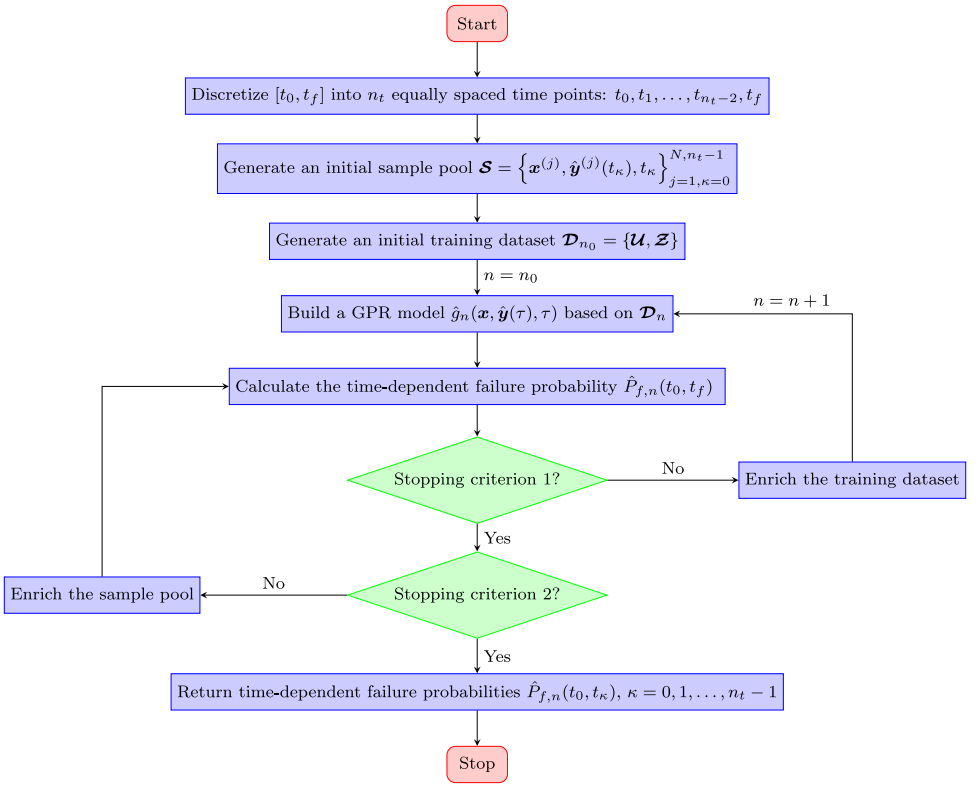


Fig. 2. Flowchart of the proposed SL-GPR-AL method.

Step 4: Build a GPR model

Build a GPR model $\hat{g}_n(\boldsymbol{x}, \hat{\boldsymbol{y}}(\tau), \tau)$ based on the data $\mathcal{D}$. In this study, we use the *fitrgp* function available in the Statistics and Machine Learning Toolbox of Matlab R2024a, with a constant prior mean and a squared exponential kernel with a separate length scale for each dimension as the prior covariance.

Step 5: Calculate the time-dependent failure probability

Calculate the time-dependent failure probability $\hat{P}_{f,n}(t_0, t_f)$ using $m_n(\boldsymbol{x}, \hat{\boldsymbol{y}}(\tau), \tau)$ through MCS with $\mathcal{S}$.

Step 6: Check the stopping criterion 1

First, calculate $\hat{P}^+_{f,n}(t_0, t_f)$ and $\hat{P}^-_{f,n}(t_0, t_f)$ using $m_n(\boldsymbol{x}, \hat{\boldsymbol{y}}(\tau), \tau)$ and $\sigma_n(\boldsymbol{x}, \hat{\boldsymbol{y}}(\tau), \tau)$ via MCS with $\mathcal{S}$. If $\frac{|\hat{P}^+_{f,n}(t_0,t_f) - \hat{P}^-_{f,n}(t_0,t_f)|}{\hat{P}_{f,n}(t_0,t_f)} < \epsilon$ is satisfied twice in a row, then go to **Step 8**; otherwise, go to **Step 7**.

Step 7: Enrich the training dataset

First, calculate $\widehat{IPoM}(\tau)$ using $m_n(\boldsymbol{x}, \hat{\boldsymbol{y}}(\tau), \tau)$ and $\sigma_n(\boldsymbol{x}, \hat{\boldsymbol{y}}(\tau), \tau)$ via MCS with $\mathcal{S}$. Second, identify the best next time instant $\tau^{(n+1)}$ by Eq. (24). Third, identify $\left(\boldsymbol{x}^{(n+1)}, \hat{\boldsymbol{y}}^{(n+1)}(\tau^{(n+1)})\right)$ by Eq. (26). Fourth, obtain $z^{(n+1)} = g\left(\boldsymbol{x}^{(n+1)}, \hat{\boldsymbol{y}}^{(n+1)}(\tau^{(n+1)}), \tau^{(n+1)}\right)$. At last, enrich the current training dataset with the new data. Let $n = n + 1$ and go to **Step 4**.

Step 8: Check the stopping criterion 2

First, calculate the CoV of $\hat{P}_{f,n}(t_0, t_f)$, i.e., $\widehat{CoV}_{\hat{P}_{f,n}(t_0,t_f)}$. If $\widehat{CoV}_{\hat{P}_{f,n}(t_0,t_f)} < \delta$ is reached (δ is a user-specified threshold), proceed to **Step 10**; otherwise, go to **Step 9**.

Step 9: Enrich the sample pool

Similar to **Step 2**, generate an another sample set $\mathcal{S}^+ = \left\{\boldsymbol{x}^{(j)}, \hat{\boldsymbol{y}}^{(j)}(t_\kappa), t_\kappa\right\}$, $j = 1, 2, \ldots, N$, $\kappa = 0, 1, \ldots, n_t - 1$. Then, enrich the current sample pool with $\mathcal{S}^+$ and proceed to **Step 5**.

Step 10: Return the time-dependent failure probability

Return the current time-dependent failure probability $\hat{P}_{f,n}(t_0, t_f)$.

Remark 2. In addition to $\hat{P}_{f,n}(t_0, t_f)$, the time-dependent failure probabilities $\hat{P}_{f,n}(t_0, t_\kappa)$ for $\kappa = 0, 1, \ldots, n_t - 2$ can also be obtained through post-processing. Therefore, they are merely by-products and not guaranteed to be as accurate as $\hat{P}_{f,n}(t_0, t_f)$. To ensure their accuracy, at least the stopping criteria would need to be modified, which is beyond the scope of this study.

Table 1
Random variables and stochastic process of Example 1.

Symbol	Distribution	Mean	Standard deviation	Auto-correlation coefficient
X_1	Normal	3.50	0.25	–
X_2	Normal	3.50	0.25	–
$Y(t)$	Gaussian process	0	1	$\exp\left(-(t_2-t_1)^2\right)$

Table 2
Time-dependent failure probability results of Example 1.

Method	N_{call}	$\hat{P}_f$	$\delta_{\hat{P}_f}$	Reference
MCS	50×10^7	0.3082	0.05%	–
eSPT	51.9	0.3082	1.52%	[34]
SILK	26.25	0.3076	1.09%	–
AFPK	24.4	0.3084	2.98%	[34]
REAL	21.75	0.3093	3.21%	–
SLK-UC	17.3	0.3071	2.38%	[42]
Proposed SL-GPR-AL	14.25	0.3096	0.63%	–

Note: N_{call} = the number (for MCS) or average number (for other methods) of calls to the g-function; $\hat{P}_f$ = the estimate (for MCS) or the mean value (for other methods) of the time-dependent failure probability; $\delta_{\hat{P}_f}$ = the CoV estimate of the time-dependent failure probability.

Remark 3. Note that the input dimension in the proposed method is d_1+d_2+1, which means that each input stochastic process is only counted as a single dimension rather than n_{KL} dimensions.

Remark 4. The proposed SL-GPR-AL method can be applied not only to the performance function of the form $g(\boldsymbol{X},\boldsymbol{Y}(\tau),\tau)$, but also to $g(\boldsymbol{X},\tau)$, $g(\boldsymbol{Y}(\tau))$, $g(\boldsymbol{Y}(\tau),\tau)$ and $g(\boldsymbol{X},\boldsymbol{Y}(\tau))$. The latter cases are actually special cases of the former and can also be encountered in time-dependent reliability analysis.

4. Numerical examples

Four numerical examples are presented in this section to demonstrate the performance of the proposed SL-GPR-AL method for time-dependent reliability analysis. Unless otherwise specified, the following parameters are used: $n_0=10$, $N=10^5$, $\delta_{\text{KL}}=0.995$, $b=1.5$, $\epsilon=10\%$ and $\delta=2\%$. For comparison, several existing active learning methods are also considered including eSPT [33], SILK [32], AFPK [34], REAL [35], VARAK [40], SLK-UC and SLK-UC-SS [42]. The reference solutions for the time-dependent failure probability and failure probability function are obtained using Monte Carlo Simulation (MCS). For those active learning methods where results are generated by us, 20 independent runs are conducted, and the statistical results are reported.

4.1. Example 1: A mathematical example

The first example considers a mathematical function taken from [53]:

$$g(\boldsymbol{X},Y(t),t)=X_1^2X_2-5X_1(1+Y(t))t+\left(X_2+1\right)t^2-20, \tag{27}$$

where $t\in[t_0,t_f]=[0,1]$; X_1, X_2 and $Y(t)$ are given in Table 1. The time interval $[0,1]$ is discretized into 50 time nodes.

Table 2 shows the results of several methods (i.e., MCS, eSPT, SILK, AFPK, REAL and SL-GPR-AL) with respect to the time-dependent failure probability $\hat{P}_f(0,1)$. The reference probability of failure is taken as 0.3082 (with a CoV of 0.05%), which is given by MCS with 50×10^7 runs. All six other methods can produce failure probability mean values very close to the reference result, but the proposed SL-GPR-AL method achieves the smallest CoV (i.e., 0.63%). Furthermore, our method requires on average the smallest number of g function calls. Note that the number of initial training data is set to be 10 in the proposed method. This means that, on average, only 4.25 additional g-function evaluations are required by the proposed method in the active learning phase.

In addition to providing the failure probability estimate $\hat{P}_f(0,1)$, the proposed method can also generate the failure probability function $\hat{P}_f(0,t),t\in[0,1]$ as a byproduct. The statistical results of $\hat{P}_f(0,t)$ are shown in Fig. 3. As can be seen, the mean curve is closed to the reference given by MCS, while the mean ± standard deviation (Std Dev) bound is very narrow.

4.2. Example 2: A simple supported beam

As shown in Fig. 4, the second example involves a simple supported corroded steel beam under uniform and concentrated loading [4]. The beam has a length of $L=5$ m and its cross-section is a rectangle with initial width b_0 and height h_0. It is assumed that the cross-sectional dimensions corrode isotropically in time at a rate of $2k$ with $k=3\times10^{-5}$ m/year. The yield stress of the material is denoted by f_y. The beam is subjected to a uniform dead load $q=78500b_0h_0$ (N/m) and a dynamic live load $F(t)$ at midspan. A failure event occurs when the applied bending moment at midspan exceeds the ultimate bending moment. The corresponding

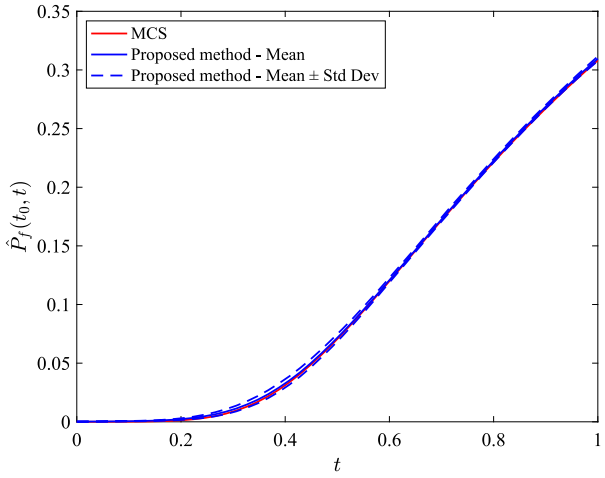


Fig. 3. Time-dependent failure probability function of Example 1.

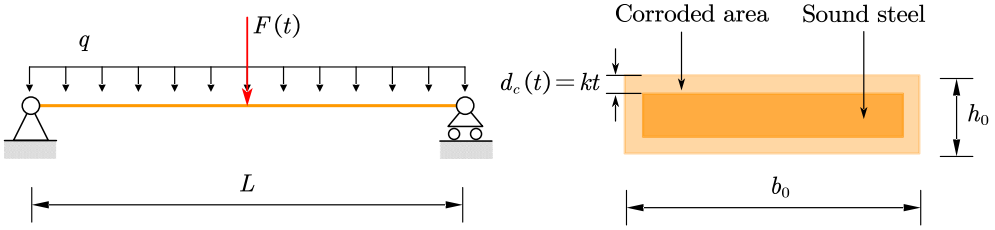


Fig. 4. A simple supported beam structure.

Table 3
Random variables and stochastic process of Example 2.

Symbol	Distribution	Mean	Standard deviation	Auto-correlation coefficient
f_y (MPa)	Lognormal	180	18	–
b_0 (m)	Lognormal	0.2	0.01	–
h_0 (m)	Lognormal	0.04	0.004	–
$F(t)$ (N)	Gaussian process	3500	700	$\exp\left(-9(t_2-t_1)^2\right)$

Table 4
Time-dependent failure probability results of Example 2.

Method	N_{call}	$\hat{P}_f$	$\delta_{\hat{P}_f}$	Reference
MCS	$200\times5\times10^6$	7.74×10^{-3}	0.51%	–
SILK	41.85	7.70×10^{-3}	1.79%	–
REAL	29.35	7.68×10^{-3}	3.31%	–
SLK-UC-SS	29.4	7.48×10^{-3}	4.08%	[42]
Proposed SL-GPR-AL	19.10	7.72×10^{-3}	2.34%	–

performance function is given by:

$$g(\boldsymbol{X},Y(t),t)=\frac{\left(b_0-2kt\right)\left(h_0-2kt\right)^2 f_y}{4}-\left(\frac{F(t)L}{4}+\frac{78500b_0h_0L^2}{8}\right), \tag{28}$$

where $t\in[t_0,t_f]=[0,10]$ years; b_0, h_0, f_y and $F(t)$ are three random variables and one stochastic process respectively, as described in Table 3. The time range of interest is discretized into 200 nodes.

The results associated with $\hat{P}_f(0,10)$ of different methods are given in Table 4. The failure probability generated by MCS is 7.74×10^{-3} (with a CoV of 0.51%), which is adopted as a reference solution. Except SLK-UC-SS, all three other methods (i.e., SILK, REAL and SL-GPR-AL) can produce failure probability means that are very close to the reference value with small CoVs. Notably, the proposed SL-GPR-AL method requires, on average, only 19.10 performance function evaluations, which is far fewer than the other three methods.

The statistical results of the time-dependent failure probability function $\hat{P}_f(0,t)$ for $t\in[0,10]$ obtained by the proposed method are shown in Fig. 5, together with the reference curve from MCS. It can be seen that the mean curve agrees well with the reference

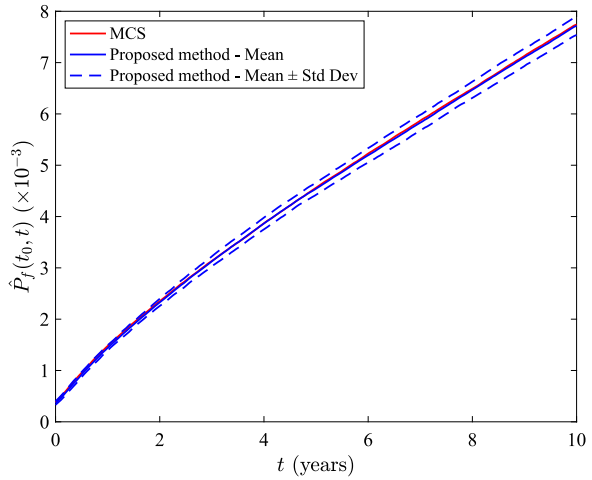


Fig. 5. Time-dependent failure probability function of Example 2.

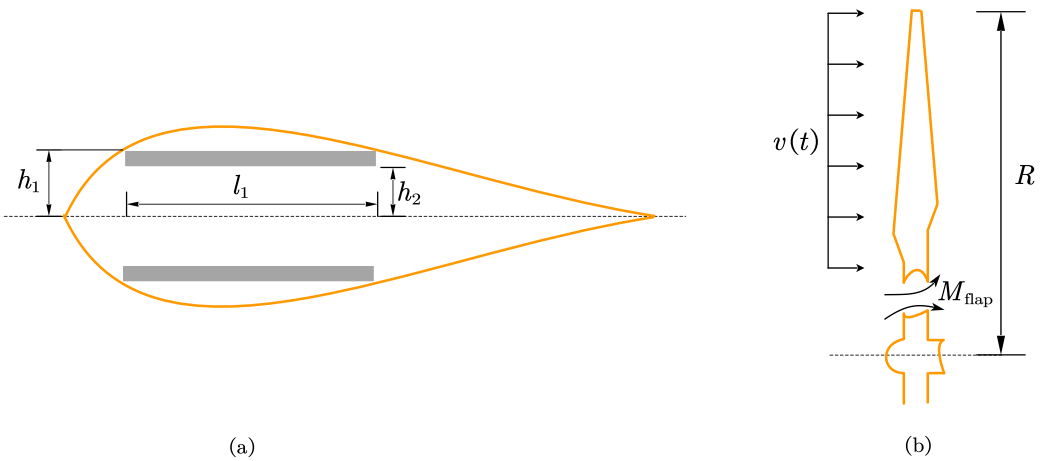


Fig. 6. A hydrokinetic turbine blade: (a) Cross section at the root of the turbine blade; (b) River flow loading on the turbine blade.

one from MCS, and the mean ± standard deviation band is quite narrow.

4.3. Example 3: A hydrokinetic turbine blade

As a third example, we consider a hydrokinetic turbine blade under a time-varying river flow load, depicted in Fig. 6. This device can convert the kinetic energy of flowing water into electrical energy. The simplified cross section at the root of the turbine blade is shown in Fig. 6(a). The width of the blade is l_1, and its height is described by h_1 and h_2. As shown in Fig. 6(b), the blade is subject to a river flow loading $v(t)$. If the bending strain at the root exceeds the allowable strain ϵ_{allow}, the blade is considered to have failed. The associated performance function is defined as:

$$g(\boldsymbol{X}, Y(t)) = \epsilon_{\text{allow}} - \frac{M_{\text{flap}} h_1}{EI}, \tag{29}$$

where $t \in [t_0, t_f] = [0, 12]$ months; $M_{\text{flap}} = \frac{1}{2}\rho v^2(t) C_{\text{m}}$ is the bending moment at the root of the blade with the water density $\rho = 1 \times 10^3$ kg/m^3 and the coefficient of moment $C_{\text{m}} = 0.3422$; $E = 14$ GPa is the Young's modulus; $I = \frac{2}{3} l_1 (h_1^3 - h_2^3)$ is the moment of inertia at the root of the blade. The random variables h_1, h_2, l_1, ϵ_{allow} and stochastic process $v(t)$ are detailed in Table 5. The time period is discretized into 200 time nodes.

The time-dependent failure probability analysis results of several different methods regarding $\hat{P}_f(0, 12)$ are listed in Table 6. The reference failure probability is 2.76×10^{-3} (with a CoV of 0.85%), obtained via MCS with $200 \times 5 \times 10^6$ runs. The four methods—eSPT, SILK, REAL and VARAK—produce fairly good failure probability results. The proposed method also yields a good failure probability mean, albeit with a slightly larger but acceptable CoV. Remarkably, the proposed method requires an average of only 15.65 performance function evaluations, which is significantly fewer than the other three methods.

Table 5
Random variables and stochastic process of Example 3.

Symbol	Distribution	Mean	Standard deviation	Auto-correlation coefficient
h_1 (m)	Normal	0.025	0.00025	–
h_2 (m)	Normal	0.019	0.00019	–
l_1 (m)	Normal	0.22	0.0022	–
ϵ_{allow}	Normal	0.025	0.00025	–
$v(t)$ (m/s)	Gaussian process	$\sum_{i=1}^{4} a_i^m \sin\left(b_i^m t + c_i^m\right)$	$\sum_{j=1}^{4} a_j^s \exp\left\{-\left[\left(t - b_j^s\right)/c_j^s\right]^2\right\}$	$\cos\left(2\pi(t_2 - t_1)\right)$

Note: The values of a_i^m, b_i^m, c_i^m, a_j^m, b_j^m and c_j^m can be found in [53].

Table 6
Time-dependent failure probability analysis results of Example 3.

Method	N_{call}	$\hat{P}_f$	$\delta_{\hat{P}_f}$	Reference
MCS	$200 \times 5 \times 10^6$	2.76×10^{-3}	0.85%	–
eSPT	52.4	2.77×10^{-3}	1.77%	[40]
SILK	36.1	2.79×10^{-3}	1.94%	[40]
REAL	29.3	2.79×10^{-3}	1.72%	[40]
VARAK	24.4	2.77×10^{-3}	1.45%	[40]
Proposed SL-GPR-AL	15.65	2.74×10^{-3}	3.78%	–

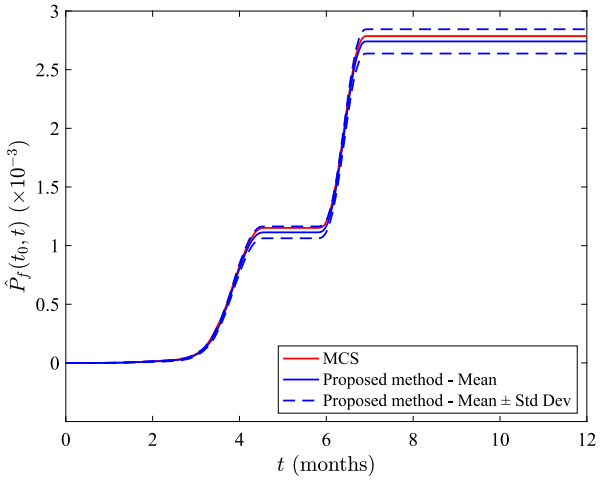


Fig. 7. Time-dependent failure probability function of Example 3.

Fig. 7 shows the statistical results regarding the time-dependent failure probability function $\hat{P}_f(0,t)$ for $t \in [0, 12]$ obtained by the proposed method, in comparison the reference solution by MCS. As can be observed, the failure probability mean curve is in good agreement with the reference, with a narrow mean ± standard deviation band.

4.4. Example 4: A space truss structure

The final example is a 120-bar space truss structure subjected to thirteen vertical loads [54], as illustrated in Fig. 8. This structure is modeled as a three-dimensional finite element model using an open-source software called OpenSees, and comprises 49 nodes and 120 truss elements. The cross-sectional area of each element is denoted by A and the modulus of elasticity of the material is denoted by E. Node 0 is subjected to a time-varying vertical concentrated load $P_0(t)$, while nodes 1 through 12 are each subjected to a time-invariant vertical concentrated load $P_1, P_2, \ldots, P_{12}$. The performance function is defined as follows:

$$g(\boldsymbol{X}, Y(t)) = \Delta - V_0(A, E, P_0(t), P_1, P_2, \ldots, P_{12}), \tag{30}$$

where $t \in [t_0, t_f] = [0, 50]$ years; V_0 denotes the vertical displacement of node 0; Δ is the corresponding threshold, which is specified as 100 mm. The involved random variables and stochastic process are given in Table 7. The time range of interest is discretized into 20 nodes.

The results for the time-dependent failure probability $\hat{P}_f(0, 50)$ are shown in Table 8. The reference failure probability is 2.11×10^{-2} with a CoV of 0.96%, given by MCS with $20 \times 5 \times 10^5$ runs. In this example, we are unable to obtain the results of SILK and REAL, as they encountered out-of-memory errors before reaching their respective stopping criteria. The proposed SL-GPR-AL method works well and produces a failure probability mean of 2.12×10^{-2} with a CoV of 2.29%. Note that this is achieved with an average of only

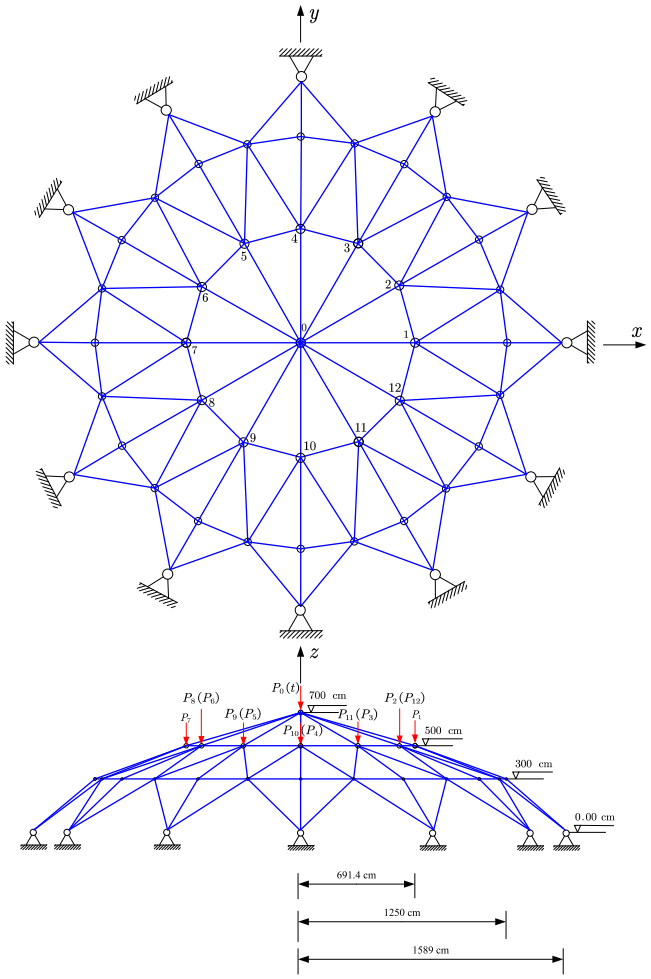


Fig. 8. A 120-bar space truss structure under vertical loads.

Table 7
Random variables and stochastic process of Example 4.

Symbol	Distribution	Mean	Standard deviation	Auto-correlation coefficient
E (GPa)	Normal	200	20	–
A (mm^2)	Normal	2000	200	–
$P_1, P_2, \ldots, P_{12}$ (kN)	Lognormal	100	15	–
$P_0(t)$ (kN)	Gaussian process	1000	150	$\exp\left(-(t_2-t_1)^2/50\right)$

Table 8
Time-dependent failure probability analysis results of Example 4.

Method	N_{call}	$\hat{P}_f$	$\delta_{\hat{P}_f}$	Reference
MCS	$20\times5\times10^5$	2.11×10^{-2}	0.96%	–
SILK	–	–	–	–
REAL	–	–	–	–
Proposed SL-GPR-AL	37.95	2.12×10^{-2}	2.29%	–

37.95 g-function evaluations.

In addition, the proposed method can also yield the time-dependent failure probability function $\hat{P}_f(0,t)$ for $t \in [0,50]$ as a byproduct. The statistical results are depicted in Fig. 9. As shown, the mean failure probability curve agrees well with the reference one obtained by MCS, with a fairly narrow mean $\pm$ standard deviation band.

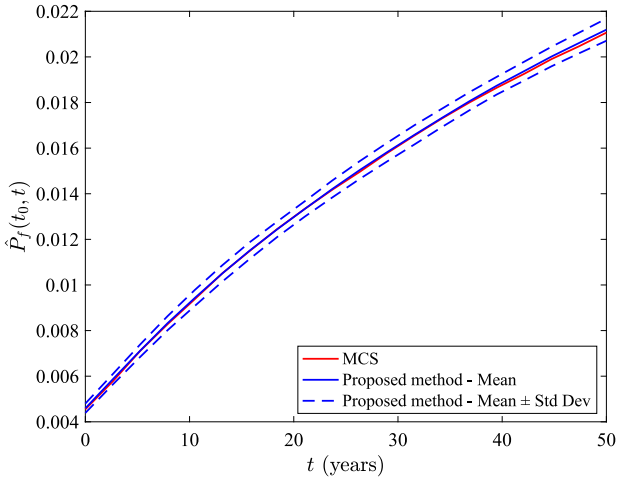


Fig. 9. Time-dependent failure probability function of Example 4.

5. Concluding remarks

This paper presents a single-loop Gaussian process regression-based active learning (AL-GPR-AL) method for time-dependent reliability analysis involving costly performance functions. The main idea is to replace an expensive-to-evaluate performance function with a GPR model built in an active learning fashion. To achieve this, we propose a novel stopping criterion using the credible bounds of the GPR model which can assess its convergence in estimating the time-dependent failure probability over a given period. In addition, we also introduce new learning functions based on the concept of misjudgment probability, which allow the identification of the most informative next points for further refinement of the GPR model when the stopping criterion cannot be satisfied. The time-dependent failure probability can be obtained from the well-trained GPR model in conjunction with Monte Carlo simulation, as well as the evolution of the failure probability as a byproduct. Besides, the proposed method can be applied to performance functions, regardless whether they are subjected to stochastic processes or not. It is empirically observed from four numerical examples that our method is able to produce accurate time-dependent failure probability results with a small number of performance function evaluations.

It is important to note that there is still potential to further improve the performance of the proposed approach. First, for assessing small time-dependent failure probabilities, Monte Carlo simulation can be replaced by more efficient methods. Second, developing suitable dimension-reduction techniques is crucial for effectively handling high-dimensional problems. Third, to increase computational efficiency, multiple points could be identified in each iteration to take advantage of parallel computing. These areas present promising directions for future research.

CRediT authorship contribution statement

Chao Dang: Writing – review & editing, Writing – original draft, Validation, Software, Methodology, Investigation, Formal analysis, Conceptualization. **Marcos A. Valdebenito:** Writing – review & editing, Validation, Conceptualization. **Matthias G.R. Faes:** Writing – review & editing, Supervision, Project administration, Funding acquisition.

Declaration of competing interest

The authors declare that they have no known competing financial interests or personal relationships that could have appeared to influence the work reported in this paper.

Acknowledgment

Chao Dang is grateful for the financial support of the German Research Foundation (DFG) (Grant number 530326817).

Data availability

No data was used for the research described in the article.

References

[1] C. Wang, M. Beer, B.M. Ayyub, Time-dependent reliability of aging structures: Overview of assessment methods, ASCE-ASME J. Risk Uncertain. Eng. Syst. A 7 (4) (2021) 03121003, http://dx.doi.org/10.1061/AJRUA6.0001176.

[2] B. Zhang, W. Wang, Y. Wang, Y. Li, C.-Q. Li, A critical review on methods for time-dependent structural reliability, Sustain. Resilient Infrastruct. 9 (2) (2024) 91–106, http://dx.doi.org/10.1080/23789689.2023.2206297.

[3] S.O. Rice, Mathematical analysis of random noise, Bell Syst. Tech. J. 23 (3) (1944) 282–332, http://dx.doi.org/10.1002/j.1538-7305.1944.tb00874.x.

[4] C. Andrieu-Renaud, B. Sudret, M. Lemaire, The phi2 method: a way to compute time-variant reliability, Reliab. Eng. Syst. Saf. 84 (1) (2004) 75–86, http://dx.doi.org/10.1016/j.ress.2003.10.005.

[5] B. Sudret, Analytical derivation of the outcrossing rate in time-variant reliability problems, Struct. Infrastruct. Eng. 4 (5) (2008) 353–362, http://dx.doi.org/10.1080/15732470701270058.

[6] X.-Y. Zhang, Z.-H. Lu, S.-Y. Wu, Y.-G. Zhao, An efficient method for time-variant reliability including finite element analysis, Reliab. Eng. Syst. Saf. 210 (2021) 107534, http://dx.doi.org/10.1016/j.ress.2021.107534.

[7] B. Zhang, W. Wang, H. Lei, X. Hu, C.-Q. Li, An improved analytical solution to outcrossing rate for scalar nonstationary and non-gaussian processes, Reliab. Eng. Syst. Saf. 247 (2024) 110102, http://dx.doi.org/10.1016/j.ress.2024.110102.

[8] C.-Q. Li, A. Firouzi, W. Yang, Closed-form solution to first passage probability for nonstationary lognormal processes, J. Eng. Mech. 142 (12) (2016) 04016103, http://dx.doi.org/10.1061/(ASCE)EM.1943-7889.0001160.

[9] A. Firouzi, W. Yang, C.-Q. Li, Efficient solution for calculation of upcrossing rate of nonstationary gaussian process, J. Eng. Mech. 144 (4) (2018) 04018015, http://dx.doi.org/10.1061/(ASCE)EM.1943-7889.0001420.

[10] Z. Hu, X. Du, Time-dependent reliability analysis with joint upcrossing rates, Struct. Multidiscip. Optim. 48 (2013) 893–907, http://dx.doi.org/10.1007/s00158-013-0937-2.

[11] C. Wang, Stochastic process-based structural reliability considering correlation between upcrossings, ASCE-ASME J. Risk Uncertain. Eng. Syst. A 6 (4) (2020) 06020002, http://dx.doi.org/10.1061/AJRUA6.0001093.

[12] C. Jiang, X. Huang, X. Han, D. Zhang, A time-variant reliability analysis method based on stochastic process discretization, J. Mech. Des. 136 (9) (2014) 091009, http://dx.doi.org/10.1115/1.4027865.

[13] Z.P. Mourelatos, M. Majcher, V. Pandey, I. Baseski, Time-dependent reliability analysis using the total probability theorem, J. Mech. Des. 137 (3) (2015) 031405, http://dx.doi.org/10.1115/1.4029326.

[14] C. Jiang, X. Wei, B. Wu, Z. Huang, An improved trpd method for time-variant reliability analysis, Struct. Multidiscip. Optim. 58 (5) (2018) 1935–1946, http://dx.doi.org/10.1007/s00158-018-2002-7.

[15] C. Gong, D.M. Frangopol, An efficient time-dependent reliability method, Struct. Saf. 81 (2019) 101864, http://dx.doi.org/10.1016/j.strusafe.2019.05.001.

[16] X. Yuan, S. Liu, M. Faes, M.A. Valdebenito, M. Beer, An efficient importance sampling approach for reliability analysis of time-variant structures subject to time-dependent stochastic load, Mech. Syst. Signal Process. 159 (2021) 107699, http://dx.doi.org/10.1016/j.ymssp.2021.107699.

[17] X. Yuan, Y. Shu, Y. Qian, Y. Dong, Adaptive importance sampling approach for structural time-variant reliability analysis, Struct. Saf. 111 (2024) 102500, http://dx.doi.org/10.1016/j.strusafe.2024.102500.

[18] H.-S. Li, T. Wang, J.-Y. Yuan, H. Zhang, A sampling-based method for high-dimensional time-variant reliability analysis, Mech. Syst. Signal Process. 126 (2019) 505–520, http://dx.doi.org/10.1016/j.ymssp.2019.02.050.

[19] W. Du, Y. Luo, Y. Wang, Time-variant reliability analysis using the parallel subset simulation, Reliab. Eng. Syst. Saf. 182 (2019) 250–257, http://dx.doi.org/10.1016/j.ress.2018.10.016.

[20] S. Chakraborty, S. Tesfamariam, Subset simulation based approach for space–time-dependent system reliability analysis of corroding pipelines, Struct. Saf. 90 (2021) 102073, http://dx.doi.org/10.1016/j.strusafe.2020.102073.

[21] M.A. Valdebenito, P. Wei, J. Song, M. Beer, M. Broggi, Failure probability estimation of a class of series systems by multidomain line sampling, Reliab. Eng. Syst. Saf. 213 (2021) 107673, http://dx.doi.org/10.1016/j.ress.2021.107673.

[22] X. Yuan, W. Zheng, C. Zhao, M.A. Valdebenito, M.G. Faes, Y. Dong, Line sampling for time-variant failure probability estimation using an adaptive combination approach, Reliab. Eng. Syst. Saf. 243 (2024) 109885, http://dx.doi.org/10.1016/j.ress.2023.109885.

[23] M. Ping, X. Han, C. Jiang, X. Xiao, A time-variant extreme-value event evolution method for time-variant reliability analysis, Mech. Syst. Signal Process. 130 (2019) 333–348, http://dx.doi.org/10.1016/j.ymssp.2019.05.009.

[24] Y. Zhang, J. Xu, M. Beer, A single-loop time-variant reliability evaluation via a decoupling strategy and probability distribution reconstruction, Reliab. Eng. Syst. Saf. 232 (2023) 109031, http://dx.doi.org/10.1016/j.ress.2022.109031.

[25] Y. Zhang, J. Xu, P. Gardoni, A loading contribution degree analysis-based strategy for time-variant reliability analysis of structures under multiple loading stochastic processes, Reliab. Eng. Syst. Saf. 243 (2024) 109833, http://dx.doi.org/10.1016/j.ress.2023.109833.

[26] Z. Wang, P. Wang, A nested extreme response surface approach for time-dependent reliability-based design optimization, J. Mech. Des. 134 (12) (2012) 121007, http://dx.doi.org/10.1115/1.4007931.

[27] Z. Wang, P. Wang, A new approach for reliability analysis with time-variant performance characteristics, Reliab. Eng. Syst. Saf. 115 (2013) 70–81, http://dx.doi.org/10.1016/j.ress.2013.02.017.

[28] Z. Hu, X. Du, Mixed efficient global optimization for time-dependent reliability analysis, J. Mech. Des. 137 (5) (2015) 051401, http://dx.doi.org/10.1115/1.4029520.

[29] C. Ling, Z. Lu, X. Zhu, Efficient methods by active learning kriging coupled with variance reduction based sampling methods for time-dependent failure probability, Reliab. Eng. Syst. Saf. 188 (2019) 23–35, http://dx.doi.org/10.1016/j.ress.2019.03.004.

[30] J. Wu, Z. Jiang, H. Song, L. Wan, F. Huang, Parallel efficient global optimization method: a novel approach for time-dependent reliability analysis and applications, Expert Syst. Appl. 184 (2021) 115494, http://dx.doi.org/10.1016/j.eswa.2021.115494.

[31] H. Li, Z. Lu, K. Feng, A double-loop kriging model algorithm combined with importance sampling for time-dependent reliability analysis, Eng. Comput. (2023) 1–20, http://dx.doi.org/10.1007/s00366-023-01879-8.

[32] Z. Hu, S. Mahadevan, A single-loop kriging surrogate modeling for time-dependent reliability analysis, J. Mech. Des. 138 (6) (2016) 061406, http://dx.doi.org/10.1115/1.4033428.

[33] Z. Wang, W. Chen, Time-variant reliability assessment through equivalent stochastic process transformation, Reliab. Eng. Syst. Saf. 152 (2016) 166–175, http://dx.doi.org/10.1016/j.ress.2016.02.008.

[34] C. Jiang, D. Wang, H. Qiu, L. Gao, L. Chen, Z. Yang, An active failure-pursuing kriging modeling method for time-dependent reliability analysis, Mech. Syst. Signal Process. 129 (2019) 112–129, http://dx.doi.org/10.1016/j.ymssp.2019.04.034.

[35] C. Jiang, H. Qiu, L. Gao, D. Wang, Z. Yang, L. Chen, Real-time estimation error-guided active learning kriging method for time-dependent reliability analysis, Appl. Math. Model. 77 (2020) 82–98, http://dx.doi.org/10.1016/j.apm.2019.06.035.

[36] H.-M. Qian, H.-Z. Huang, Y.-F. Li, A novel single-loop procedure for time-variant reliability analysis based on kriging model, Appl. Math. Model. 75 (2019) 735–748, http://dx.doi.org/10.1016/j.apm.2019.07.006.

[37] Y. Yan, J. Wang, Y. Zhang, Z. Sun, Kriging model for time-dependent reliability: accuracy measure and efficient time-dependent reliability analysis method, IEEE Access 8 (2020) 172362–172378, http://dx.doi.org/10.1109/ACCESS.2020.3014238.

[38] Y. Hu, Z. Lu, N. Wei, C. Zhou, A single-loop kriging surrogate model method by considering the first failure instant for time-dependent reliability analysis and safety lifetime analysis, Mech. Syst. Signal Process. 145 (2020) 106963, http://dx.doi.org/10.1016/j.ymssp.2020.106963.
[39] D. Wang, H. Qiu, L. Gao, C. Jiang, A single-loop kriging coupled with subset simulation for time-dependent reliability analysis, Reliab. Eng. Syst. Saf. 216 (2021) 107931, http://dx.doi.org/10.1016/j.ress.2021.107931.
[40] Z. Song, H. Zhang, L. Zhang, Z. Liu, P. Zhu, An estimation variance reduction-guided adaptive kriging method for efficient time-variant structural reliability analysis, Mech. Syst. Signal Process. 178 (2022) 109322, http://dx.doi.org/10.1016/j.ymssp.2022.109322.
[41] R. Cao, Z. Sun, J. Wang, F. Guo, A single-loop reliability analysis strategy for time-dependent problems with small failure probability, Reliab. Eng. Syst. Saf. 219 (2022) 108230, http://dx.doi.org/10.1016/j.ress.2021.108230.
[42] F. Hong, P. Wei, J. Fu, Y. Xu, W. Gao, A new acquisition function combined with subset simulation for active learning of small and time-dependent failure probability, Struct. Multidiscip. Optim. 66 (4) (2023) 72, http://dx.doi.org/10.1007/s00158-023-03531-x.
[43] S. Huang, S. Quek, K. Phoon, Convergence study of the truncated karhunen–loeve expansion for simulation of stochastic processes, Internat. J. Numer. Methods Engrg. 52 (9) (2001) 1029–1043, http://dx.doi.org/10.1002/nme.255.
[44] C.-C. Li, A. Der Kiureghian, Optimal discretization of random fields, J. Eng. Mech. 119 (6) (1993) 1136–1154, http://dx.doi.org/10.1061/(ASCE)0733-9399(1993)119:6(1136).
[45] M. Shinozuka, G. Deodatis, Simulation of Stochastic Processes by Spectral Representation, Appl. Mech. Rev. 44 (4) (1991) 191–204, http://dx.doi.org/10.1115/1.3119501.
[46] J. Chen, W. Sun, J. Li, J. Xu, Stochastic harmonic function representation of stochastic processes, J. Appl. Mech. 80 (1) (2013) 011001, http://dx.doi.org/10.1115/1.4006936.
[47] C.K. Williams, C.E. Rasmussen, Gaussian Processes for Machine Learning, MIT Press, Cambridge, MA, 2006.
[48] R. Schöbi, B. Sudret, S. Marelli, Rare event estimation using polynomial-chaos kriging, ASCE-ASME J. Risk Uncertain. Eng. Syst. A 3 (2) (2017) D4016002, http://dx.doi.org/10.1061/AJRUA6.0000870.
[49] Y. Shi, Z. Lu, L. Xu, S. Chen, An adaptive multiple-kriging-surrogate method for time-dependent reliability analysis, Appl. Math. Model. 70 (2019) 545–571, http://dx.doi.org/10.1016/j.apm.2019.01.040.
[50] B. Echard, N. Gayton, M. Lemaire, AK-MCS: an active learning reliability method combining Kriging and Monte Carlo simulation, Struct. Saf. 33 (2) (2011) 145–154, http://dx.doi.org/10.1016/j.strusafe.2011.01.002.
[51] C. Dang, M.A. Valdebenito, M.G. Faes, P. Wei, M. Beer, Structural reliability analysis: A Bayesian perspective, Struct. Saf. 99 (2022) 102259, http://dx.doi.org/10.1016/j.strusafe.2022.102259.
[52] C. Dang, M. Beer, Semi-Bayesian active learning quadrature for estimating extremely low failure probabilities, Reliab. Eng. Syst. Saf. 246 (2024) 110052, http://dx.doi.org/10.1016/j.ress.2024.110052.
[53] Z. Wang, W. Chen, Confidence-based adaptive extreme response surface for time-variant reliability analysis under random excitation, Struct. Saf. 64 (2017) 76–86, http://dx.doi.org/10.1016/j.strusafe.2016.10.001.
[54] C. Dang, P. Wei, J. Song, M. Beer, Estimation of failure probability function under imprecise probabilities by active learning–augmented probabilistic integration, ASCE-ASME J. Risk Uncertain. Eng. Syst. A 7 (4) (2021) 04021054, http://dx.doi.org/10.1061/AJRUA6.0001179.